Chinese Journal of Aeronautics 25 (2012) 252-261

Contents lists available at ScienceDirect

Chinese Journal of Aeronautics

journal homepage: www.elsevier.com/locate/cja

Track-before-detect for Infrared Maneuvering Dim Multi-target via MM-PHD

LONG Yunli, XU Hui, AN Wei*, LIU Li

College of Electronic Science and Engineering, National University of Defense Technology, Changsha 410073, China

Received 26 May 2011; revised 2 September 2011; accepted 19 December 2011

Abstract

In this paper, we present a novel and efficient track-before-detect (TBD) algorithm based on multiple-model probability hypothesis density (MM-PHD) for tracking infrared maneuvering dim multi-target. Firstly, the standard sequential Monte Carlo probability hypothesis density (SMC-PHD) TBD-based algorithm is introduced and sequentially improved by the adaptive process noise and the importance re-sampling on particle likelihood, which result in the improvement in the algorithm robustness and convergence speed. Secondly, backward recursion of SMC-PHD is derived in order to ameliorate the tracking performance especially at the time of the multi-target arising. Finally, SMC-PHD is extended with multiple-model to track maneuvering dim multi-target. Extensive experiments have proved the efficiency of the presented algorithm in tracking infrared maneuvering dim multi-target, which produces better performance in track detection and tracking than other TBD-based algorithms including SMC-PHD, multiple-model particle filter (MM-PF), histogram probability multi-hypothesis tracking (H-PMHT) and Viterbi-like.

Keywords: target tracking; probability hypothesis density; Monte Carlo; track-before-detect; importance re-sampling

1. Introduction

The problem of detecting and tracking infrared maneuvering dim multi-target at low signal-to-noise ratio (SNR) is very challenging and has received great attention in the last several years. An approach, referred as track-before-detect (TBD), jointly processes raw data from several consecutive frames and declares the presence of the target and eventually its track, which outperforms traditional algorithms at the price of an increase of computational complexity. Many TBD- based algorithms have been proposed such as histogram probability multi-hypothesis tracking (H-PMHT) [1-2], particle filter (PF) [3-6] and so on. Davey and Rutten [7] proves that PF outperforms H-PMHT and probabilistic data association (PDA) [8] regardless of computation cost. PF is proposed for the single target scenarios and is combined with multiple-model (MM-PF) to track the maneuvering one. Although it can be modified for multi-target scenarios by composite multi-hypothesis testing or heuristic searching [9], it is complex and time consuming. An efficient Viterbi-like algorithm based on generalized likelihood ratio test (GLRT) is presented [10] for detecting a moving target by airborne radar. Sequentially it is extended for multi-target scenarios via dynamic programming or via an equivalent minimum network flow optimization when the target number N_k at time step k is a priori known. And suboptimum algorithms are proposed, which separate the original joint maximization problem into N_k reduced dimension disjoint optimizations and extract multi-target one by one similarly to heuristic searching. When the target number N_k is unknown, the more challenging problem of tracking and detecting multi-target can be solved by composite multi-hypothesis testing [11]. However, the algorithms presented in Refs. [10]-[11] do not incorporate the target kine-

*Corresponding author. Tel.: +86-731-84573489.
E-mail address: nudtanwei@tom.com
Foundation item: Ministry Level Project

doi: 10.1016/S1000-9361(11)60385-3

matics, but simply consider a maximum target velocity to define the admissible target transitions. The derivation in Ref. [10] is extended in the context of space-time adaptive processing (STAP) [12]. A one-step GLRT-based detector for the scan-to-scan varying scenario and ad hoc detectors for both stationary and varying scenarios are derived. And then it is further extended for bistatic sonars [13] and advanced by taking into account possible spillover of target energy and incorporating the target kinematics [14]. Although the derivation in Ref. [12] and Ref. [14] could be extended to multi-target scenarios with the target number unknown by introducing composite multi-hypothesis testing, it would become very complex and not work well when the targets are number-varying and maneuvering.

Fortunately, probability hypothesis density (PHD) has been proposed based on random finite set for tracking multi-target [15], which can efficiently estimate the target number and state simultaneously. A sequential Monte Carlo PHD (SMC-PHD) is designed by Vo, et al. [16] and multiple-model PHD (MM-PHD) [17] is presented consequently for maneuvering targets on a set of point measurement, which has been extensively applied in tracking targets for sonars, radars and so on. An SMC-PHD TBD-based algorithm is proposed to track low-observable multi-target [18]. However, it does poorly in tracking targets at their coming-up stage and especially in tracking maneuvering ones. Therefore we present an MM-PHD TBD-based algorithm for tracking maneuvering dim targets.

2. Dynamic and Measurement Models for Targets

The dynamics of the tth target is generally given by

$$\boldsymbol{X}_k^{(t)} = \boldsymbol{F}^{(r)}(\boldsymbol{X}_{k-1}^{(t)}) + \boldsymbol{v}_k^r \quad (t=1,2,\cdots,N_k; r=1,2,\cdots,N_r) \tag{1}$$

where $\boldsymbol{X}_k^{(t)}$ denotes the tth target state on the focal plane at time step k, $\boldsymbol{F}^{(r)}$ the state transition function with the superscript r representing the dynamic model index parameter, $\boldsymbol{v}_k^r$ the normal random noise vector with zero mean and covariance matrix $\boldsymbol{Q}_k^r$, N_k the target number surviving at time step k and N_r the number of the dynamic models introduced. $\boldsymbol{F}^{(r)}$ and $\boldsymbol{Q}_k^r$ are both defined in Ref. [7] and Ref. [19] for the constant velocity (CV or constant acceleration (CA)) and the clockwise/anticlockwise coordinated turn (C-CT/AC-CT) target dynamics. Usually the dynamic models of the target evolve as a Markov chain with transition probabilities matrix $\boldsymbol{\Pi}$. If the tth target exercises a CV dynamic model, $\boldsymbol{X}_k^{(t)} \in \mathbf{R}^{5\times 1}$ is given as

$$\boldsymbol{X}_k^{(t)} = \left[x_k^{(t)} \quad \dot{x}_k^{(t)} \quad y_k^{(t)} \quad \dot{y}_k^{(t)} \quad I^{(t)} \right]^{\mathrm{T}} \tag{2}$$

where $(x_k^{(t)}, y_k^{(t)})$, $(\dot{x}_k^{(t)}, \dot{y}_k^{(t)})$ and $I^{(t)}$ respectively denote the target position, velocity and intensity at time step k. For a CA dynamic model, the target acceleration $(\ddot{x}_k^{(t)}, \ddot{y}_k^{(t)})$ is further included.

The sensor provides two-dimensional images of the surveillance region at an interval of T seconds and each image consists of $N\times M$ resolution cells. Each cell corresponds to a rectangular region of dimensions $\Delta_x\times\Delta_y$ (Δ_x, $\Delta_y\in\mathbf{R}$) and the center of each cell (i, j) (i=1, 2, ···, N; j=1, 2, ···, M) is defined to be at $((i-0.5)\Delta_x, (j-0.5)\Delta_y)$. The measured intensity $z_k^{(i,j)} \in \mathbf{R}$ at the cell (i, j) is given as

$$z_k^{(i,j)} = \begin{cases} \sum_{t=1}^{N_k} h_k^{(i,j)}(\boldsymbol{X}_k^{(t)}, \boldsymbol{u}_k) + n_k^{(i,j)}, & H_1 \\ n_k^{(i,j)}, & H_0 \end{cases} \tag{3}$$

where H_1 means N_k targets present with H_0 denoting no target, $n_k^{(i,j)}$ is assumed to be the Gaussian measurement noise with variance σ_{n}^2 and independent from cell to cell and from image to image, $\boldsymbol{u}_k=[\Delta_k^x \quad \Delta_k^y]^{\mathrm{T}}$ ($\boldsymbol{u}_k\in\mathbf{R}^{2\times 1}$) the imaging position errors in two dimensions due to disturbance. The contribution of the tth target to the cell (i, j) at time step k, i.e. $h_k^{(i,j)}$, is given by [20]

$$h_k^{(i,j)}\left(\boldsymbol{X}_k^{(t)}, \boldsymbol{u}_k\right) = \int_{(i-1)\Delta_x}^{i\Delta_x}\int_{(j-1)\Delta_y}^{j\Delta_y} \frac{I^{(t)}}{2\pi\Sigma^2} \cdot \exp\left(\frac{-\left(x - x_k^{(t)} - \Delta_k^x\right)^2 - \left(y - y_k^{(t)} - \Delta_k^y\right)^2}{2\Sigma^2} \right) \mathrm{d}x\mathrm{d}y \tag{4}$$

where $\Sigma\in\mathbf{R}$ represents the amount of blurring introduced by the sensor. The peak SNR of the tth target is given by

$$\mathrm{SNR} = 20\lg[I^{(t)}/(2\pi\sigma_{\mathrm{n}}\Sigma^2)]\ \mathrm{dB} \tag{5}$$

The measurements at time step k are given by $z_k = \{z_k^{(i,j)}: i=1, 2, \cdots, N; j=1, 2, \cdots, M\}$ and the set of measurements up to time step k is $Z_k=\{z_m: m=1, 2, \cdots, k\}$. The likelihood of the measurements at time step k is formulated as

$$p\left(z_k \middle| \boldsymbol{X}_k^{(1)}, \boldsymbol{X}_k^{(2)}, \cdots, \boldsymbol{X}_k^{(N_k)}\right) = \begin{cases} \prod_{i=1}^{N}\prod_{j=1}^{M} p_{s+n}\left(z_k^{(i,j)} \middle| \boldsymbol{X}_k^{(1)}, \boldsymbol{X}_k^{(2)}, \cdots, \boldsymbol{X}_k^{(N_k)}\right), & H_1 \\ \prod_{i=1}^{N}\prod_{j=1}^{M} p_n\left(z_k^{(i,j)}\right), & H_0 \end{cases} \tag{6}$$

where

$$\begin{cases} p_{s+n}\left(z_k^{(i,j)} \middle| \boldsymbol{X}_k^{(1)}, \boldsymbol{X}_k^{(2)}, \cdots, \boldsymbol{X}_k^{(N_k)}\right) = \mathcal{N}\left(z_k^{(i,j)}; \sum_{t=1}^{N_k} h_k^{(i,j)}\left(\boldsymbol{X}_k^{(t)}, \boldsymbol{u}_k\right), \sigma_{\mathrm{n}}^2\right) \\ p_n\left(z_k^{(i,j)}\right) = \mathcal{N}\left(z_k^{(i,j)}; 0, \sigma_{\mathrm{n}}^2\right) \end{cases} \tag{7}$$

where $\mathcal{N}(\bullet; \mu,\sigma^2)$ denotes the Gaussian probability density with mean μ and variance σ^2.

3. SMC-PHD TBD and Its Improvement

3.1. SMC-PHD TBD

The SMC-PHD TBD-based algorithm is proposed by Punithakumar, et al. [18] to track low-observable multi-target. Let the posterior density $D_{k-1}(\boldsymbol{X}_{k-1}|\boldsymbol{Z}_{k-1})$ be represented at time step $k-1$ by a set of particles $\{\boldsymbol{X}_{k-1}^p\}_{p=1}^{L_{k-1}}$ with particle weights $\{w_{k-1}^p\}_{p=1}^{L_{k-1}}$:

$$D_{k-1}\left(\boldsymbol{X}_{k-1}\left|\boldsymbol{Z}_{k-1}\right.\right)=\sum_{p=1}^{L_{k-1}} w_{k-1}^p \delta\left(\boldsymbol{X}_{k-1}-\boldsymbol{X}_{k-1}^p\right) \quad (8)$$

where $\boldsymbol{X}_{k-1}$ denotes the state vector, $\boldsymbol{X}_{k-1}^p$ that of the pth particle at time step $k-1$ with its weight w_{k-1}^p, L_{k-1} the number of particles surviving at time step $k-1$ and $\delta(\bullet)$ the Dirac delta function. $\boldsymbol{X}_{k-1}$ in PHD should be interpreted as an accumulated (or compressed) multi-target rather than as a conventional single-target state [21]. According to the derivation in Ref. [18], the SMC-PHD TBD-based algorithm processes as follows.

1) Prediction

According to the proposal density $q_k\left(\bullet|\boldsymbol{X}_{k-1}^p,\boldsymbol{Z}_k\right)$ and $p_k\left(\bullet|\boldsymbol{Z}_k\right)$, generate L_{k-1} samples for surviving targets and J_k samples for new-born targets respectively:

$$\boldsymbol{X}_{k|k-1}^p \sim \begin{cases} q_k\left(\bullet\left|\boldsymbol{X}_{k-1}^p,\boldsymbol{Z}_k\right.\right), & p=1,2,\cdots,L_{k-1} \\ p_k\left(\bullet\left|\boldsymbol{Z}_k\right.\right), & p=L_{k-1}+1,L_{k-1}+2,\cdots,L_{k-1}+J_k \end{cases} \quad (9)$$

And the predicted density is approximated by

$$D_{k|k-1}\left(\boldsymbol{X}_{k|k-1}\left|\boldsymbol{Z}_{k-1}\right.\right)=\sum_{p=1}^{L_{k-1}+J_k} w_{k|k-1}^p \delta\left(\boldsymbol{X}_{k|k-1}-\boldsymbol{X}_{k|k-1}^p\right) \quad (10)$$

where the predicted weights are given as

$$w_{k|k-1}^p=\begin{cases} \left[e_{k|k-1}\left(\boldsymbol{X}_{k-1}^p\right)f_k\left(\boldsymbol{X}_{k|k-1}^p\left|\boldsymbol{X}_{k-1}^p\right.\right)\Big/q_k\left(\boldsymbol{X}_{k|k-1}^p\left|\boldsymbol{X}_{k-1}^p,\boldsymbol{Z}_k\right.\right)+\right. \\ \left. b_{k|k-1}\left(\boldsymbol{X}_{k|k-1}^p\left|\boldsymbol{X}_{k-1}^p\right.\right)\Big/q_k\left(\boldsymbol{X}_{k|k-1}^p\left|\boldsymbol{X}_{k-1}^p,\boldsymbol{Z}_k\right.\right)\right]w_k^p, \\ \qquad p=1,2,\cdots,L_{k-1} \\ \gamma_k\left(\boldsymbol{X}_{k|k-1}^p\right)\Big/\left[J_k p_k\left(\boldsymbol{X}_{k|k-1}^p\left|\boldsymbol{Z}_k\right.\right)\right], \\ \qquad p=L_{k-1}+1,L_{k-1}+2,\cdots,L_{k-1}+J_k \end{cases} \quad (11)$$

where $f_k(\bullet)$ denotes the target state transition density, $e_{k|k-1}(\bullet)$ the probability that the target would survive at time step k, $b_{k|k-1}(\bullet)$ the PHD of the spawned target, and $\gamma_k(\bullet)$ the PHD of the spontaneous target.

2) Updating

Usually the cell (i, j) is not functioned by more than one target if the targets are sufficiently spaced apart from one another, i.e. $\forall\, t, t' \in [1, N_k], t \neq t'$:

$$\left(x_k^{(t)}-x_k^{(t')}\right)^2+\left(y_k^{(t)}-y_k^{(t')}\right)^2 \geq (6\Sigma)^2 \quad (12)$$

Therefore the likelihood ratio of the measurement intensity $z_k^{(i,j)}$ functioned by a target with the particle state $\boldsymbol{X}_k^p$ is given as

$$l\left(z_k^{(i,j)}\left|\boldsymbol{X}_k^p\right.\right)\triangleq p_{s+n}\left(z_k^{(i,j)}\left|\boldsymbol{X}_k^p\right.\right)\Big/p_n\left(z_k^{(i,j)}\right)= \exp\left\{-\frac{h_k^{(i,j)}\left(\boldsymbol{X}_k^p,\boldsymbol{u}_k\right)\left(h_k^{(i,j)}\left(\boldsymbol{X}_k^p,\boldsymbol{u}_k\right)-2z_k^{(i,j)}\right)}{2\sigma_{\mathrm{n}}^2}\right\} \quad (13)$$

Then the updated weight $\tilde{w}_k^p$ for the particle p at time step k can be calculated by

$$\tilde{w}_k^p=\frac{\prod_{i\in C_i\left(\boldsymbol{X}_{k|k-1}^p\right)}\prod_{j\in C_j\left(\boldsymbol{X}_{k|k-1}^p\right)} l\left(z_k^{(i,j)}\left|\boldsymbol{X}_{k|k-1}^p\right.\right)w_{k|k-1}^p}{\lambda_k+\Psi_k\left(z_k^{(i_0,j_0)}\left(\boldsymbol{X}_{k|k-1}^p\right)\right)} \left(i_0=\mathbb{D}_i\left(\boldsymbol{X}_{k|k-1}^p\right), j_0=\mathbb{D}_j\left(\boldsymbol{X}_{k|k-1}^p\right)\right) \quad (14)$$

where λ_k is a normalized constant and $\Psi_k(\bullet)$ is given by

$$\Psi_k\left(z_k^{(i_0,j_0)}\left(\boldsymbol{X}_{k|k-1}^p\right)\right)= \sum_{p\in P^{(i_0,j_0)}} w_{k|k-1}^p \prod_{i\in C_i\left(\boldsymbol{X}_{k|k-1}^p\right)}\prod_{j\in C_j\left(\boldsymbol{X}_{k|k-1}^p\right)} l\left(z_k^{(i,j)}\left|\boldsymbol{X}_{k|k-1}^p\right.\right) \quad (15)$$

$$P^{(i_0,j_0)}=\left\{p: p\in[1,L_{k-1}+J_k]\left|i_0=\mathbb{D}_i\left(\boldsymbol{X}_{k|k-1}^p\right),\right.\right. \left.\left. j_0=\mathbb{D}_j\left(\boldsymbol{X}_{k|k-1}^p\right)\right\}\right. \quad (16)$$

The cell mostly influenced by the target is defined as

$$\begin{cases} \mathbb{D}_i\left(\boldsymbol{X}_{k|k-1}^p\right)=\max\limits_i h_k^{(i,j)}\left(\boldsymbol{X}_{k|k-1}^p,\boldsymbol{u}_k\right) \\ \mathbb{D}_j\left(\boldsymbol{X}_{k|k-1}^p\right)=\max\limits_j h_k^{(i,j)}\left(\boldsymbol{X}_{k|k-1}^p,\boldsymbol{u}_k\right) \end{cases} \quad (17)$$

And $C_i\left(\boldsymbol{X}_{k|k-1}^p\right)$ and $C_j\left(\boldsymbol{X}_{k|k-1}^p\right)$ are the sets of subscripts i and j, respectively corresponding to cells affected by the target, which are defined by

$$\begin{cases} C_i\left(\boldsymbol{X}_{k|k-1}^p\right)=\left\{i\left|\left\|i-\mathbb{D}_i\left(\boldsymbol{X}_{k|k-1}^p\right)\right\|\leq 3\Sigma\right.\right\} \\ C_j\left(\boldsymbol{X}_{k|k-1}^p\right)=\left\{j\left|\left\|j-\mathbb{D}_j\left(\boldsymbol{X}_{k|k-1}^p\right)\right\|\leq 3\Sigma\right.\right\} \end{cases} \quad (18)$$

3) Re-sampling and multi-target state estimation

The target number is estimated by

$$\hat{n}_k^X=\sum_{p=1}^{L_{k-1}+J_k}\tilde{w}_k^p \quad (19)$$

Then re-sample the set $\{\tilde{w}_k^p/\hat{n}_k^X, \boldsymbol{X}_{k|k-1}^p\}_{p=1}^{L_{k-1}+J_k}$ to get $\{w_k^p/\hat{n}_k^X, \boldsymbol{X}_k^p\}_{p=1}^{L_k}$ with the sum of the weights $\{w_k^p\}_{p=1}^{L_k}$ remaining $\hat{n}_k^X$. The posterior density is updated by

$$D_k\left(\boldsymbol{X}_k\left|\boldsymbol{Z}_k\right.\right)=\sum_{p=1}^{L_k} w_k^p \delta\left(\boldsymbol{X}_k-\boldsymbol{X}_k^p\right) \tag{20}$$

With the estimation of the target number $\hat{n}_k^{\boldsymbol{X}}$, the particle set $\{\boldsymbol{X}_k^p\}_{p=1}^{L_k}$ is separated to $\hat{n}_k^{\boldsymbol{X}}$ classes by k-means. And the multi-target state $\{\hat{\boldsymbol{X}}_k^{(t)}\}_{t=1}^{\hat{n}_k^X}$ is sequentially extracted on the center of each class accompanied with the covariance matrix $\{\hat{\boldsymbol{P}}_k^{(t)}\}_{t=1}^{\hat{n}_k^X}$ estimated on the target state and the particles of each class.

3.2. Improvement of SMC-PHD TBD

In this section the SMC-PHD TBD-based algorithm is modified to improve its performance. Firstly, instead of the constant process noise covariance matrix, the adaptive one is adopted to enhance the robustness of the algorithm. Secondly, re-sampling of SMC-PHD is conducted on particle likelihood to speed up its convergence instead of on the updated particle weight. Finally, the backward recursive SMC-PHD is derived to improve tracking performance at the coming-up stage for the new born targets.

1) Adaptive process noise

The process noise has a great influence on the algorithm robustness. When the process noise is too small, the predicted particles are expected to concentrate on the target state. Once the target state strongly fluctuates for disturbance, the particles can hardly cover it, which results in the degradation of the performance. However, too large process noise leads to a lot of barren particles being apart from the target state. So we should choose the adaptive process noise. Given the tth target state covariance matrix at time step k and $k-1$ as $\hat{\boldsymbol{P}}_k^{(t)}$ and $\hat{\boldsymbol{P}}_{k-1}^{(t)}$, the process noise covariance matrix $\boldsymbol{Q}_{k+1}^r$ for the rth dynamic model at time step $k+1$ is adopted by

$$\boldsymbol{Q}_{k+1}^r=\begin{cases}\boldsymbol{Q}_{\min}^r+\left(\boldsymbol{Q}_k^r-\boldsymbol{Q}_{\min}^r\right)\exp\left(1-\left\|\hat{\boldsymbol{P}}_k^{(t)}\right\|\Big/\left\|\hat{\boldsymbol{P}}_{k-1}^{(t)}\right\|\right), \\ \qquad\qquad\qquad\qquad\qquad \left\|\hat{\boldsymbol{P}}_k^{(t)}\right\|\geqslant\left\|\hat{\boldsymbol{P}}_{k-1}^{(t)}\right\| \\ \boldsymbol{Q}_{\max}^r+\left(\boldsymbol{Q}_k^r-\boldsymbol{Q}_{\max}^r\right)\exp\left(1-\left\|\hat{\boldsymbol{P}}_{k-1}^{(t)}\right\|\Big/\left\|\hat{\boldsymbol{P}}_k^{(t)}\right\|\right), \\ \qquad\qquad\qquad\qquad\qquad \left\|\hat{\boldsymbol{P}}_k^{(t)}\right\|<\left\|\hat{\boldsymbol{P}}_{k-1}^{(t)}\right\|\end{cases} \tag{21}$$

where $\boldsymbol{Q}_{\min}^r$ and $\boldsymbol{Q}_{\max}^r$ respectively correspond to the minimum and the maximum of the process noise covariance matrix for the rth dynamic model, and $\left\|\hat{\boldsymbol{P}}_k^{(t)}\right\|$ denotes the determinant of the matrix $\hat{\boldsymbol{P}}_k^{(t)}$. Usually $\boldsymbol{Q}_{\min}^r$ is preset according to Ref. [19] with the level of the power spectral density $q_s=0.001$ and $\boldsymbol{Q}_{\max}^r$ is set to be $50\boldsymbol{Q}_{\min}^r$. If $\left\|\hat{\boldsymbol{P}}_k^{(t)}\right\|$ is smaller than $\left\|\hat{\boldsymbol{P}}_{k-1}^{(t)}\right\|$, it means that the particles congregate in fewer cells. Therefore $\boldsymbol{Q}_{k+1}^r$ should be enlarged to ensure that the predicted particles cover the target state at time step $k+1$. If $\left\|\hat{\boldsymbol{P}}_k^{(t)}\right\|$ is not smaller than $\left\|\hat{\boldsymbol{P}}_{k-1}^{(t)}\right\|$, it implies that there are more barren particles apart from the target. So $\boldsymbol{Q}_{k+1}^r$ should be reduced in order to focalize the predicted particles around the target at next time step $k+1$.

2) Re-sampling based on particle likelihood

The ratio of the likelihood of the particle p to that of the particle q is defined as

$$\gamma_{p,q}\triangleq\frac{p_{s+n}\left(z_k\left|\boldsymbol{X}_{k|k-1}^p\right.\right)\Big/p_n\left(z_k\right)}{p_{s+n}\left(z_k\left|\boldsymbol{X}_{k|k-1}^q\right.\right)\Big/p_n\left(z_k\right)}\approx\frac{\prod\limits_{i\in C_i\left(\boldsymbol{X}_{k|k-1}^p\right)}\prod\limits_{j\in C_j\left(\boldsymbol{X}_{k|k-1}^p\right)} l\left(z_k^{(i,j)}\left|\boldsymbol{X}_{k|k-1}^p\right.\right)}{\prod\limits_{i\in C_i\left(\boldsymbol{X}_{k|k-1}^q\right)}\prod\limits_{j\in C_j\left(\boldsymbol{X}_{k|k-1}^q\right)} l\left(z_k^{(i,j)}\left|\boldsymbol{X}_{k|k-1}^q\right.\right)} \tag{22}$$

According to Eq. (14), the ratio of the updated weights for the two particles is given as

$$\eta_{p,q}=\frac{w_k^p}{w_k^q}\propto\frac{\tilde{w}_k^p}{\tilde{w}_k^q}=\gamma_{p,q}\frac{\lambda_k+\Psi_k\left(z_k^{(i_0,j_0)}\left(\boldsymbol{X}_{k|k-1}^q\right)\right)}{\lambda_k+\Psi_k\left(z_k^{(i_0,j_0)}\left(\boldsymbol{X}_{k|k-1}^p\right)\right)} \tag{23}$$

If the pth particle corresponds to a target with the qth particle corresponding to non-target, $\eta_{p,q}$ is smaller than $\gamma_{p,q}$. If both the pth and qth particles correspond to the target, $\eta_{p,q}$ approximates $\gamma_{p,q}$. This means that it would reproduce more particles corresponding to a target based on their likelihood than on their updated weights. Therefore the importance re-sampling is implemented according to particle likelihood. With the target number $\hat{n}_k^{\boldsymbol{X}}$ being estimated on the sum of the particle weights $\{\tilde{w}_k^p\}_{p=1}^{L_k}$, the updated particle weights are redefined by

$$\tilde{w}_k'^p\propto\prod_{i\in C_i\left(\boldsymbol{X}_{k|k-1}^p\right)}\prod_{j\in C_j\left(\boldsymbol{X}_{k|k-1}^p\right)} l\left(z_k^{(i,j)}\left|\boldsymbol{X}_{k|k-1}^p\right.\right) \tag{24}$$

Then re-sample the particle set $\{w_{k|k-1}^p,\boldsymbol{X}_{k|k-1}^p\}_{p=1}^{L_{k-1}+J_k}$ to get $\{w_k^p/\hat{n}_k^{\boldsymbol{X}},\boldsymbol{X}_k^p\}_{p=1}^{L_k}$ with the sum of the weights amounting to $\hat{n}_k^{\boldsymbol{X}}$.

3) Backward recursion of SMC-PHD

Without prior information, the particles sampled for the new born targets are usually generated uniformly over the surveillance cells, which converge to the target state via re-sampling after several frames. Therefore we propose the backward recursion of SMC-PHD to improve tracking performance at the target coming-up stage, which is implemented to the new born targets once it is detected.

Assume the target number estimated at time step k_0 to be $\hat{n}_{k_0}^{X}$. Let $\hat{\boldsymbol{X}}_{k_0}^{(t)}$ and $\hat{\boldsymbol{P}}_{k_0}^{(t)}$ be the tth target state and its covariance matrix extracted by k-means. The particles are re-selected by a gate ξ to be $\{\{\boldsymbol{X}_{k_0}^{p}\}_{p=1}^{L_{k_0}^{(t)}}\}_{t=1}^{\hat{n}_{k_0}^{X}}$ with weights $\{\{w_{k_0}^{p}\}_{p=1}^{L_{k_0}^{(t)}}\}_{t=1}^{\hat{n}_{k_0}^{X}}$:

$$\left\{\boldsymbol{X}_{k_0}^{p}\right\}_{p=1}^{L_{k_0}^{(t)}}=\left\{\boldsymbol{X}_{k_0}^{p}\left|\left(\boldsymbol{X}_{k_0}^{p}-\hat{\boldsymbol{X}}_{k_0}^{(t)}\right)^{\mathrm{T}}\left(\hat{\boldsymbol{P}}_{k_0}^{(t)}\right)^{-1}\cdot\left(\boldsymbol{X}_{k_0}^{p}-\hat{\boldsymbol{X}}_{k_0}^{(t)}\right)\le\xi, p=1,2,\cdots,L_{k_0}\right.\right\} \tag{25}$$

where $L_{k_0}^{(t)}$ is the number of particles re-selected corresponding to the tth target. From the time step $k=k_0$ to $k=1$, the backward recursive SMC-PHD for the tth target works as follows:

(a) Generate $L_k^{(t)}$ samples for the surviving target from the proposal density $q_{k-1}(\bullet|\boldsymbol{X}_k^p,\boldsymbol{Z}_k)$:

$$\boldsymbol{X}_{k-1|k}^{p}\sim q_{k-1}(\bullet|\boldsymbol{X}_k^p,\boldsymbol{Z}_k),\ p=1,2,\cdots,L_k^{(t)} \tag{26}$$

(b) Given neither spawned nor spontaneous target, the back-predicted weights are given by

$$w_{k-1|k}^{p}=\frac{e_{k-1|k}\left(\boldsymbol{X}_k^p\right)f_{k-1}\left(\boldsymbol{X}_{k-1|k}^{p}\left|\boldsymbol{X}_k^p\right.\right)}{q_{k-1}\left(\boldsymbol{X}_{k-1|k}^{p}\left|\boldsymbol{X}_k^p,\boldsymbol{Z}_k\right.\right)} \tag{27}$$

(c) Then the particle weights $\{\tilde{w}_{k-1}^{p}\}_{p=1}^{L_k^{(t)}}$ and the posterior density $D_{k-1}(\boldsymbol{X}_{k-1}|\boldsymbol{Z}_k)$ for the tth target can be updated according to Eqs. (14)-(20). And particles are re-sampled by Eq. (24) consequently with the target state being extracted by k-means.

4. MM-PHD TBD and Its Implementation

The SMC-PHD TBD-based algorithm is proposed for tracking dim multi-target with a certain dynamic model. However, it performs poorly to track the maneuvering ones with the uncertain dynamic model. Therefore the MM-PHD TBD-based algorithm is proposed in this section for tracking maneuvering dim multi-target based on the combination of the improved SMC-PHD TBD-based algorithm and multiple-model [17]. Given the number of the dynamic models as N_r, the proposal model density for new born targets as β_k and that for surviving targets as Ξ_k, the transition probability matrix for the dynamic models as $\boldsymbol{\Pi}$, the MM-PHD TBD-based algorithm is initialized at time step k=1 as follows:

1) As to the proposal model density β_1, generate J_1 samples:

$$r_1^p\sim\beta_1(\bullet),\ p=1,2,\cdots,J_1 \tag{28}$$

2) Generate J_1 particles according to the proposal density $p_1(\bullet|\boldsymbol{Z}_1)$:

$$\boldsymbol{X}_1^p\sim p_1(\bullet|\boldsymbol{Z}_1),\quad p=1,2,\cdots,J_1 \tag{29}$$

For particle position components, the proposal density is uniform over the cells $\{z_1^{(i,j)}|z_1^{(i,j)}\ge\mathrm{Th}\}$, where Th is a predefined threshold value. For particle intensity components, the density is uniform between $[I_{\min}, I_{\max}]$, where $I_{\min}$ and $I_{\max}$ are the minimum and maximum target intensity levels respectively. For particle velocity components, the density is uniform between $[-V_{\max}, V_{\max}]$ pixel/s, where $V_{\max}$ is the maximum target speed.

3) The particle weights are given as

$$w_1^p=\gamma_1/J_1,\qquad p=1,2,\cdots,J_1 \tag{30}$$

And the density $D_1(\boldsymbol{X}_1|\boldsymbol{Z}_1)$ is represented by the set of particles $\{\boldsymbol{X}_{k-1}^p, r_1^p, w_1^p\}_{p=1}^{J_1}$. From time step k=2, the MM-PHD TBD-based algorithm works as follows.

4.1. Prediction

1) Generate samples according to the model proposal density:

$$r_{k|k-1}^{p}\sim\begin{cases}\Xi_k\left(\bullet\left|r_{k-1}^{p}\right.\right), & p=1,2,\cdots,L_{k-1}\\ \beta_k(\bullet),\ p=L_{k-1}+1,L_{k-1}+2,\cdots,L_{k-1}+J_k\end{cases} \tag{31}$$

where r_{k-1}^{p} is the model index parameter for the pth particle at time step $k-1$ with the predicted $r_{k|k-1}^{p}$ at time step k.

2) Generate samples according to its proposal density and model parameter:

$$\boldsymbol{X}_{k|k-1}^{p}\sim\begin{cases}q_k\left(\bullet\left|\boldsymbol{X}_{k-1}^{p},r_{k|k-1}^{p},\boldsymbol{Z}_k\right.\right), & p=1,2,\cdots,L_{k-1}\\ p_k\left(\bullet\left|r_{k|k-1}^{p},\boldsymbol{Z}_k\right.\right), & p=L_{k-1}+1,L_{k-1}+2,\cdots,L_{k-1}+J_k\end{cases} \tag{32}$$

The predicted particle weights can be calculated by

$$w_{k|k-1}^{p}=\begin{cases}\left[\dfrac{e_{k|k-1}\left(\boldsymbol{X}_{k-1}^{p}\right)f_k\left(\boldsymbol{X}_{k|k-1}^{p}\left|\boldsymbol{X}_{k-1}^{p},r_{k|k-1}^{p}\right.\right)}{q_k\left(\boldsymbol{X}_{k|k-1}^{p}\left|\boldsymbol{X}_{k-1}^{p},r_{k|k-1}^{p},\boldsymbol{Z}_k\right.\right)}+\dfrac{b_{k|k-1}\left(\boldsymbol{X}_{k|k-1}^{p}\left|\boldsymbol{X}_{k-1}^{p},r_{k|k-1}^{p}\right.\right)}{q_k\left(\boldsymbol{X}_{k|k-1}^{p}\left|\boldsymbol{X}_{k-1}^{p},r_{k|k-1}^{p},\boldsymbol{Z}_k\right.\right)}\right]\cdot\dfrac{\boldsymbol{\Pi}\left(r_{k|k-1}^{p}\left|r_{k-1}^{p}\right.\right)}{\Xi_k\left(r_{k|k-1}^{p}\left|r_{k-1}^{p}\right.\right)}w_{k-1}^{p}, & p=1,2,\cdots,L_{k-1}\\ \dfrac{\gamma_k\left(\boldsymbol{X}_{k|k-1}^{p}\left|r_{k|k-1}^{p}\right.\right)}{J_k\ p_k\left(\boldsymbol{X}_{k|k-1}^{p}\left|r_{k|k-1}^{p},\boldsymbol{Z}_k\right.\right)}\cdot\dfrac{\theta_k\left(r_{k|k-1}^{p}\right)}{\beta_k\left(r_{k|k-1}^{p}\right)}, & p=L_{k-1}+1,L_{k-1}+2,\cdots,L_{k-1}+J_k\end{cases} \tag{33}$$

where the probability mass function $\theta_k(\bullet)$ denotes the model distribution of spontaneously born targets at time step k. And the proposal density for the target state, model and the probability mass function can be chosen by

$$\begin{cases} q_k\left(\bullet\middle|\boldsymbol{X}_{k-1}^p, r_{k|k-1}^p, \boldsymbol{Z}_k\right)=f_k\left(\bullet\middle|\boldsymbol{X}_{k-1}^p, r_{k|k-1}^p\right) \\ \Xi_k\left(\bullet\middle|r_{k-1}^p\right)=\boldsymbol{\Pi}\left(\bullet\middle|r_{k-1}^p\right) \\ \theta_k\left(r_{k|k-1}^p\right)=\beta_k\left(r_{k|k-1}^p\right) \end{cases} \tag{34}$$

4.2. Updating, re-sampling and multi-target state estimation

The updating and importance re-sampling are similar to those of the improved SMC-PHD detailed by the Eqs. (14)-(24). The target number and state are estimated according to Eqs. (19)-(20). The probability $P_{k,r}^{(t)}$ for the tth target with the model index parameter r at time step k is estimated by

$$P_{k,r}^{(t)}=L_{k,r}^{(t)}\Big/L_k^{(t)} \tag{35}$$

where $L_k^{(t)}$ is the number of particles corresponding to the tth target at time step k, and $L_{k,r}^{(t)}$ the number of its particles with the model index parameter r.

The MM-PHD TBD-based algorithm is implemented to track low-observable maneuvering multi-target as illustrated in Fig. 1. Firstly, an MM-PHD TBD detector is constructed to capture new-born multi-target. And then MM-PHD TBD trackers are built for each new-born target detected, which works only for tracking the surviving target without regard to neither spawned nor spontaneous target. A track for the detected target will not be established and confirmed until it is tracked for three frames continuously. Once a track is set up, the backward MM-PHD TBD tracker is implemented. Both the forward and backward recursive MM-PHD TBD trackers halt if the track has been dropped continuously for two frames. Furthermore, the measurement data z_k for the detector is modified on the tracked multi-target state for fear of establishing the captured tracks once more.

As illustrated in Fig. 1, $k_0^{N_k}$ is the time instant at which the N_kth target is captured and $\hat{\boldsymbol{X}}_{k_0^{N_k}:k-1}^{(N_k)}$ represents its state from the time step $k_0^{N_k}$ to $k-1$ with $\hat{\boldsymbol{P}}_{k_0^{N_k}:k-1}^{(N_k)}$ denoting the corresponding covariance matrix. The measurement z_k is modified for the detector by

$$z_k^*=\left\{z_k\middle|z_k^{(i,j)}=I_0,\forall(i,j)\in \bigcup_{t=1}^{N_k}\left\{(n,m)\middle|n\in C_i\left(\hat{\boldsymbol{X}}_k^{(t)}\right),m\in C_j\left(\hat{\boldsymbol{X}}_k^{(t)}\right)\right\}\right\} \tag{36}$$

where the constant I_0 is set to be $-3\ \sigma_n$.

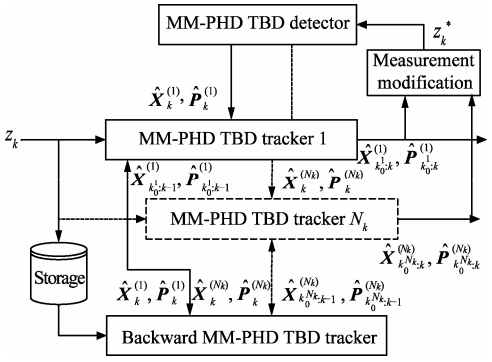

Fig. 1 Diagram of MM-PHD TBD-based algorithm.

5. Simulations and Results

5.1. Comparison of the standard and improved SMC-PHD

Firstly, the improved SMC-PHD TBD-based algorithm is compared with the standard one in scenarios with one target at different SNR, which appears at 5 s with the initial state [5 pixel, 0.9 pixel/s, 5 pixel, 0.2 pixel/s, I^t] and moves at constant velocity for 20 s to disappear. The target intensity I^t is given by

$$I^t=2\pi\sigma_n\Sigma^2\times10^{\mathrm{SNR}/20} \tag{37}$$

The frequency of the frame is 1 Hz and the image consists of 40×40(N×M) resolution cells with the resolution Δx=Δy=1. The noise variance σ_n^2 is set to be 1 and the position error in each dimension is Gaussian distributed with standard deviation 0.5 pixel. The initial process noise is kept the same as Ref. [7] with the power spectral density parameters q_s=0.001 and q_i=0.01. The minimum of the particle intensity $I_{\min}$ is set to be $0.8I^t$ with the maximum $I_{\max}$ set as $1.2I^t$. The maximum of particle speed $V_{\max}$ is set to be 4 pixel/s. The Monte Carlo number M_c is set to be 100. Other related parameter values are listed in Table 1.

Table 1 Parameter values for simulations

Σ	J_k	e_k	b_k	γ_k	$L_k^{\max}$	SNR/dB		
0.7	2 000	0.99	0	0.05	4 000	12	10	8

In order to reduce the complexity, the raw measurement z_k is pre-segmented by a very low threshold Th to get the cells, in which multi-target might locate. And as to Eq. (9) and Eq. (29) the particles sampled for new born targets are uniformly distributed around the cells. The threshold Th is adopted on SNR to ensure that the multi-target is detected with the probability p_d=0.99 at every frame. And the constant λ_k in Eq. (14) is set to be $1-\Phi(\mathrm{Th}/\sigma_n)$, where Φ denotes the normal Gaussian cumulative distribution function.

The performance is evaluated on root mean square error (RMSE) of the target position in the focal plane

and optimal sub-pattern assignment (OSPA) [22], which depicts the estimation performance of both the target number and state. RMSE of the *t*th target position at time step *k* is defined as

$$\mathrm{RMSE}(t,k)=\sqrt{\frac{1}{M_{\mathrm{c}}}\sum_{n=1}^{M_{\mathrm{c}}}\left[\left(x_k^{(t)}-\hat{x}_{k,n}^{(t)}\right)^2+\left(y_k^{(t)}-\hat{y}_{k,n}^{(t)}\right)^2\right]} \quad (38)$$

where $\left(\hat{x}_{k,n}^{(t)},\hat{y}_{k,n}^{(t)}\right)$ denotes the target position estimated at the *n*th simulation. OSPA and RMSE for the standard and improved SMC-PHD are shown in Fig. 2. It can be seen that the improved SMC-PHD gives better performance. As SNR increases, the difference between the two algorithms dwindles. The reason might be that the target particles are reproduced much more by the re-sampling based on the likelihood than on the updated weights, which leads to the faster convergence and better OSPA and RMSE.

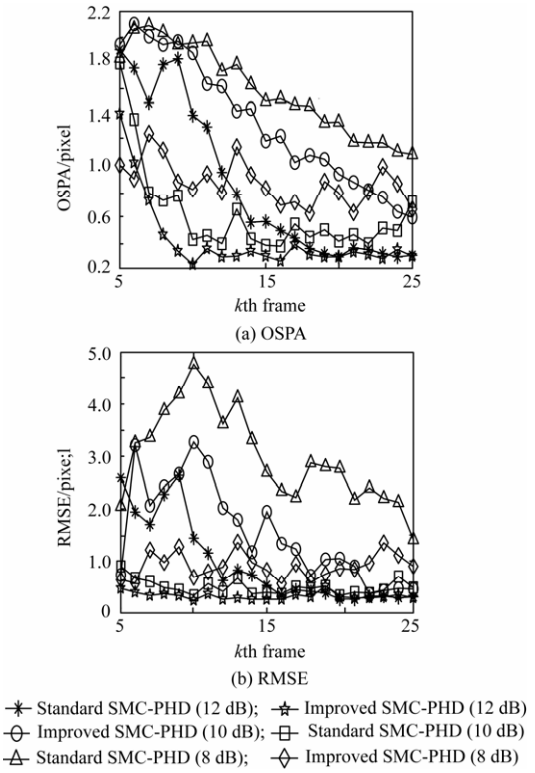

Fig. 2 OSPA and RMSE of target position for the standard and improved SMC-PHD.

5.2. MM-PHD for maneuvering dim targets

The MM-PHD TBD-based algorithm is tested on the scenario with three targets at SNR 10 dB, which consists of 40 frame data at an interval of T=1 s. Target 1 appears at the 5th frame with the initial state [15 pixel 1.5 pixels/s 10 pixel 0 pixel/s 9.74]$^{\mathrm{T}}$, moves for 10 s in a CV model and then switches to an AC-CT model for 10 s. Afterwards it switches to a CV model again for 10 s and vanishes at the 35th frame. Target 2 arises at the 5th frame with the initial state [25 pixel −1.3 pixels/s 18 pixel 0 pixel/s 9.74]$^{\mathrm{T}}$, moves for 10 s in a CV model and then switches to a C-CT model for the next 10 s. And it switches to CV again for 10 s and disappears at the 35th frame. Target 3 moves in a CV model from the 10 th frame to the 30th frame with the initial state [20 pixel 0 pixel/s 35 pixel −1.5 pixel/s 9.74]$^{\mathrm{T}}$. The probability for the new born target with the CV, C-CT and AC-CT model is respectively set to be 0.8, 0.1 and 0.1. Markov model transition probabilities matrix $\boldsymbol{\Pi}$ is given as

$$\boldsymbol{\Pi}=\begin{bmatrix}0.8 & 0.1 & 0.1\\ 0.3 & 0.6 & 0.1\\ 0.3 & 0.1 & 0.6\end{bmatrix} \quad (39)$$

Other parameter values are the same with those in Table 1. The simulated data at the 10th frame is shown in Fig. 3(a), and the true tracks and the tracked are plotted in Fig. 3(b). OSPA and RMSE of target position for all the three targets are shown in Fig. 4. The estimated model probability for the targets at different time steps is plotted in Fig. 5.

Simulation results show that MM-PHD can successfully track the maneuvering dim targets with the exact estimation of the dynamic model probability.

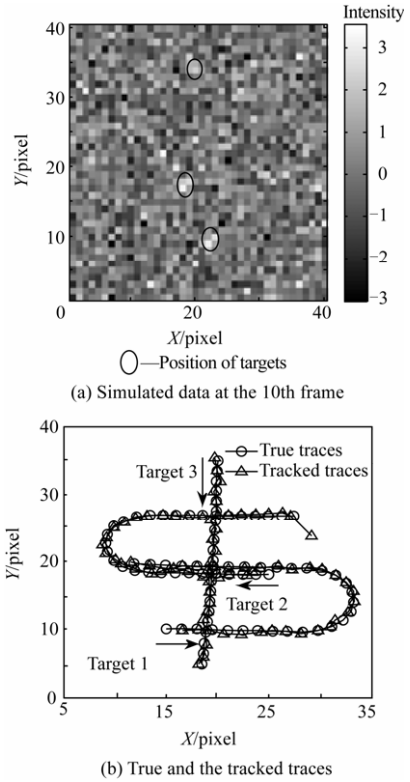

Fig. 3 Simulated data, true and the tracked traces.

5.3. Comparison of TBD-based algorithms

In this section the performances of TBD-based algorithms for tracking multi-target by space-based optical sensors are compared, including MM-PHD, heuristic

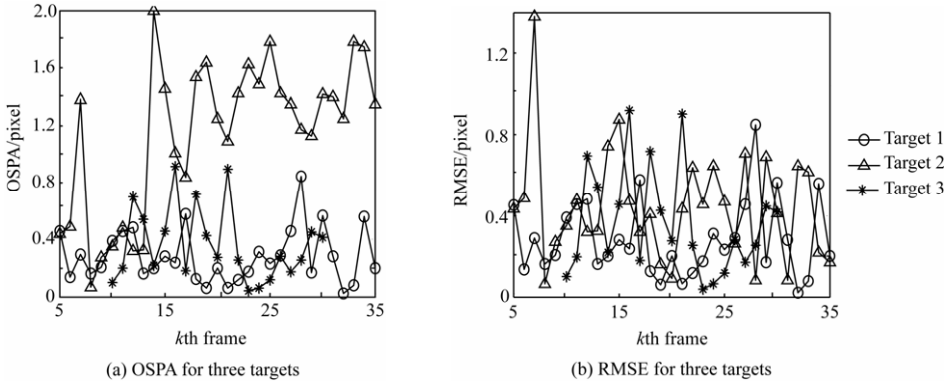

Fig. 4 OSPA and RMSE of position estimation for targets.

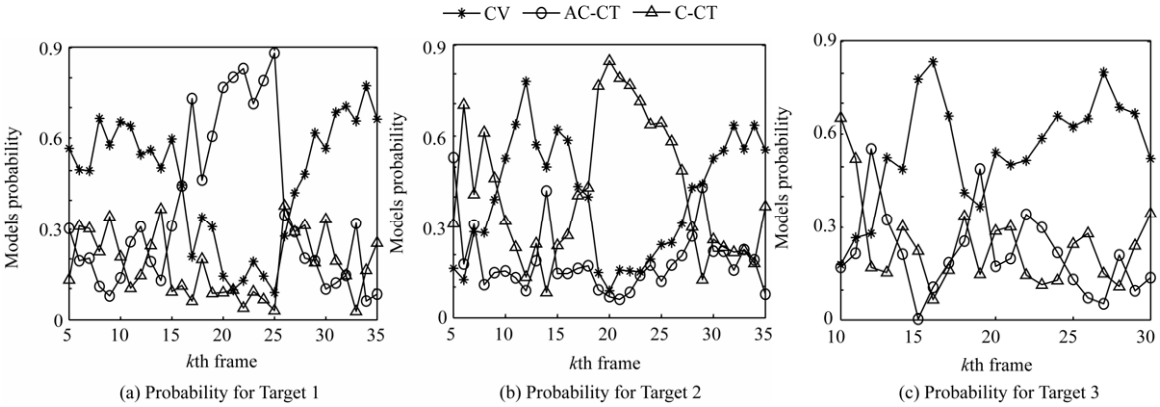

Fig. 5 Models probability estimated for three targets.

MM-PF [3,9,23], H-PMHT [7] and Viterbi-like [24]. The scenario consists of 42 frame data at the frequency 0.5 Hz with three maneuvering targets generated by STK. Targets 1–2 are launched at the 8th frame with SNR 13 dB and Target 3 is launched at the 15th frame with SNR 11 dB. Other parameter values are N=80, M=100, Σ=0.6, J_k=5 000 with the missing probability P_M=0.05, the false probability $P_F=10^{-5}$ for the likelihood ratio testing in MM-PF [3]. The procedure of the Viterbi-like algorithm is depicted in Ref. [24], wherein the target velocity is limited with the range [−3, 3] pixels/s in each of the x and y directions and the target kinematics is incorporated for the recursion with the position uncertainty of 2 pixels in two dimensions. In order to process 42 frame data, a sliding windowed algorithm is implemented with the window length 8 and a threshold V_T is set to be 11.3 to confirm the tentative target track path. The track paths are extracted once their scores exceed V_T and their trajectories are estimated by backward tracking. In addition to the CA model for SMC-PHD, H-PMHT and Viterbi-like, C-CT and AC-CT models are introduced for MM-PHD and MM-PF.

The experiment is conducted for 100 times. Simulated data at the 10th frame and the tracks are respectively shown in Figs. 6 (a)-(b).

The performances of track detection and tracking are shown in Table 2 and Figs. 7-8. Wherein the probabil-

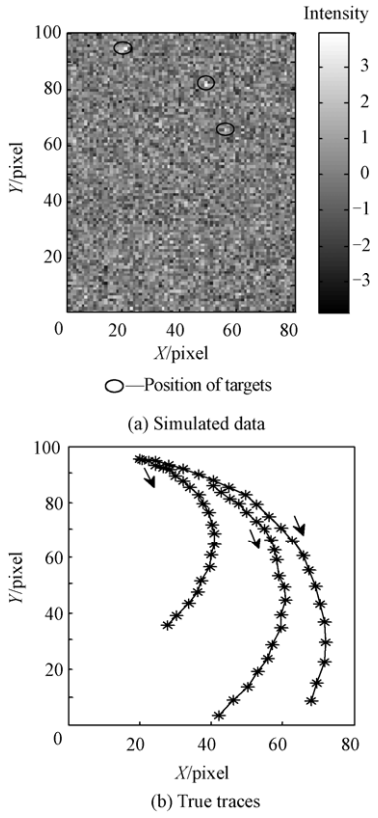

Fig. 6 Simulated data and true traces.

Table 2 Performance of track detection

TBD-based algorithm	Probability of tracks detection P_{TD}/%	False tracks accepted
Heuristic MM-PF	94.3	1
MM-PHD	95.3	0
SMC-PHD	92.7	0
Viterbi-like	60.0	21
H-PMHT	41.0	3

ity of tracks detection P_{TD} is defined as the probability that the correct target number is declared and their tracks are initialized within the accuracy of 5 pixels.

From Table 2 and Figs. 7-8, it can be seen that the presented MM-PHD TBD-based algorithm successfully tracks the maneuvering dim multi-target with the highest track detection probability and tracking accuracy. The former three algorithms are effective with a little difference in performance, which are implemented by particle filtering to solve the nonlinear esti-

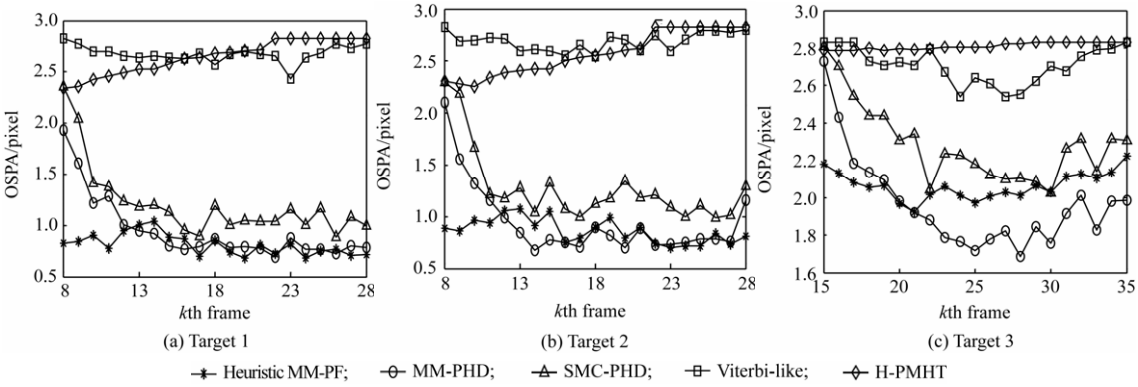

Fig. 7 OSPA for multi-target.

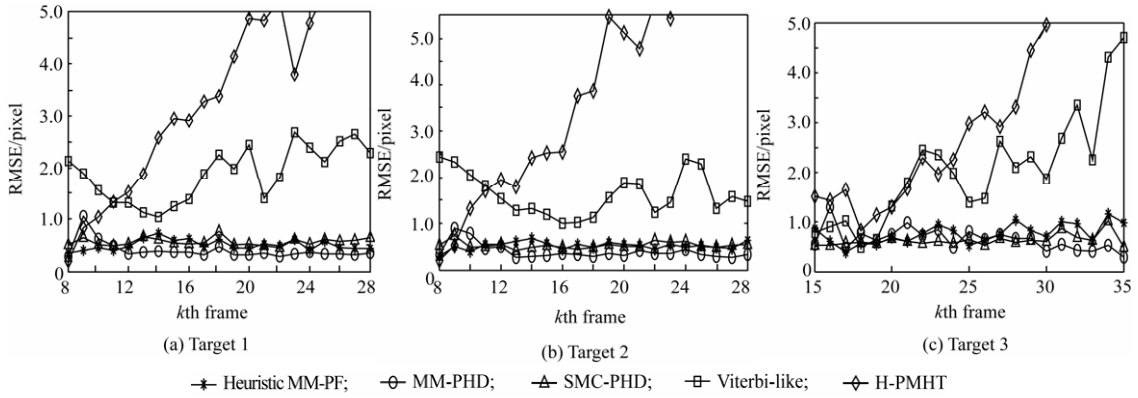

Fig. 8 RMSE of position estimation for multi-target.

mation problem, while H-PMHT and Viterbi-like perform poorly. However, several targets are dropped by all the former three algorithms. It may be due to the limited particles generated for the new born targets, which are not sampled enough to completely cover the true state of targets. The performance would be improved by increasing J_k at the cost of an increase of the computation.

Furthermore, MM-PHD while the time tracks being detected and terminated is compared with SMC-PHD and heuristic MM-PF. From Table 3 and Table 4, it can be seen that the presented MM-PHD algorithm captures the new born targets and terminates the vanished ones as soon as possible.

Table 3 Time of tracks being detected

TBD-based algorithm	Time/frame		
	Target 1	Target 2	Target 3
MM-PHD	10.7	10.2	20.6
Heuristic MM-PF	14.7	14.3	24.7
SMC-PHD	10.9	10.3	20.8

Table 4 Time of tracks being halted

TBD-based algorithm	Time/frame		
	Target 1	Target 2	Target 3
MM-PHD	31.2	31.3	36.3
Heuristic MM-PF	33.5	34.5	37.2
SMC-PHD	31.4	31.3	35.7

6. Conclusions

In this paper, we propose an MM-PHD TBD-based algorithm on the combination of the improved SMC-PHD and multiple-model for tracking maneuvering dim multi-target. Experiments show that the proposed algorithm can effectively track maneuvering dim multi-

target with better performance than other algorithms including SMC-PHD, heuristic MM-PF TBD, H-PMHT and Viterbi-like.

Acknowledgement

The authors wish to thank Dr. Danilo Orlando (Università del Salento, Italy) for his helpful comments and constructive suggestions.

References

[1] Streit R L, Graham M L, Walsh M J. Multitarget tracking of distributed targets using histogram-PMHT. Digital Signal Processing 2002; 12(2-3): 394-404.
[2] Efe M, Parkfiliz A G. Multi-target tracking in clutter with histogram probabilistic multi-hypothesis tracker. International Conference on Systems Engineering. 2005; 137-142.
[3] Boers Y, Driessen H. A particle filter based detection scheme. IEEE Signal Processing Letters 2003; 10(10): 300-302.
[4] Rutten M G, Gordona N J, Maskell S. Efficient particle-based track-before-detect in Rayleigh noise. The 7th International Conference on Information Fusion. 2004; 693-700.
[5] Salmond D J, Birch H. A particle filter for track-before-detect. Proceedings of American Control Conference. 2001; 3755-3760.
[6] Boers Y, Driessen J N. Multitarget particle filter track before detect application. IEE Proceedings—Radar, Sonar and Navigation 2004; 151(6): 351-357.
[7] Davey S J, Rutten M G. A comparison of three algorithms for tracking dim targets. International Conference on Information, Decision and Control. 2007: 342-347.
[8] Kirubarajan T, Barshalom Y. Probabilistic data association techniques for target tracking in clutter. Proceedings of IEEE 2004; 92(3): 536-557.
[9] Pertil P. A track before detect approach for sequential Bayesian tracking of multiple speech sources. International Conference on Acoustics Speech and Signal Processing. 2010; 4974-4977.
[10] Buzzi S, Lops M, Venturino L. Track-before-detect procedures for early detection of moving target from airbone radars. IEEE Transactions on Aerospace and Electronic Systems 2005; 41(3): 937-954.
[11] Buzzi S, Lops M, Venturino L, et al. Track-before-detect procedures in a multi-target environment. IEEE Transactions on Aerospace and Electronic Systems 2008; 44(3): 1150-1153.
[12] Orlando D, Venturino L, Marco L, et al. Track-before-detect strategies for STAP radars. IEEE Transactions on Signal Processing 2010; 58(2): 933-938.
[13] Orlando D, Ehlers F, Ricci G. Track-before-detect algorithms for bistatic sonars. The 2nd International Workshop on Cognitive Information Processing. 2010; 180-185.
[14] Orlando D, Ricci G, Bar-Shalom Y. Track-before-detect algorithms for targets with kinematic constraints. IEEE Transactions on Aerospace and Electronic Systems 2011; 47(3): 1837-1849.
[15] Mahler R. Multi-target Bayes filtering via first-order multi-target moments. IEEE Transaction on Aerospace and Electronic System 2003; 39(4): 1152-1178.
[16] Vo B N, Singh S S, Doucet A. Sequential Monte Carlo methods for multi-target filtering with random finite sets. IEEE Transactions on Aerospace and Electronic System 2005; 41(4): 1224-1245.
[17] Punithakumar K, Kirubarajan T, Sinha A. Multiple-model probability hypothesis density filter for tracking maneuvering targets. IEEE Transactions on Aerospace and Electronic System 2008; 44(1): 87-98.
[18] Punithakumar K, Kirubarajan T, Sinha A. A sequential Monte Carlo probability hypothesis density algorithm for multitarget track-before-detect. Proc SPIE 5913, 59131S(2005).
[19] Li X R, Jinkov V P. A survey of maneuvering target tracking—Part I: dynamic models. IEEE Transactions on Aerospace and Electronic System 2003; 39(4): 1333-1364.
[20] Deepa K, Dimitrios H. Blind image deconvolution. IEEE Signal Processing Magazine 1996; 13(3): 43-64.
[21] Mahler R. A theoretical foundation for the Stein-Winter "probability hypothesis density (PHD)" multitarget tracking approach. ADA400161, 2000.
[22] Dominic S, Batuong V, Vo B N. A consistent metric for performance evaluation of multi-object filters. IEEE Transactions on Signal Processing 2008; 56(8): 3447-3457.
[23] Boers Y, Driessen J N. Interacting multiple model particle filter. IEE Proceedings—Radar, Sonar and Navigation 2003; 150(5): 344-349.
[24] Johnston L A, Krishnamurthy V. Performance analysis of a dynamic programming track before detect algorithm. IEEE Transactions on Aerospace and Electronic System 2002; 38(1): 228-242.

Biographies:

LONG Yunli received his B.S. and M.S. degrees from the National University of Defense Technology in 2003 and 2005. Now he is working towards the Ph.D. degree with National University of Defense Technology. His research interests are multi-target detection and tracking, passive location, infrared information processing and information fusion.
E-mail: feiyunlyi@126.com

XU Hui received his Ph.D. degree from the National University of Defense Technology in 1995. Since 2005, he has been a professor at the same University. His research interests include infrared information processing, passive location and tracking, and information fusion.
E-mail: simon863@vip.sina.com